

# Multiclass Brain Tumor Classification using Region Growing based Tumor Segmentation and Ensemble Wavelet Features

Ghazanfar Latif

College of Computer Engineering and Sciences, Prince Mohammad bin Fahd University, Saudi Arabia.

[glatif@pmu.edu.sa](mailto:glatif@pmu.edu.sa)

D.N.F. Awang Iskandar

Faculty of Computer Science and Information Technology, Universiti Malaysia Sarawak, Malaysia.

[dnfaiz@unimas.my](mailto:dnfaiz@unimas.my)

Jaafar Alghazo

College of Computer Engineering and Sciences, Prince Mohammad bin Fahd University, Saudi Arabia.

[jghazo@pmu.edu.sa](mailto:jghazo@pmu.edu.sa)

## ABSTRACT

In this research, an automated method is proposed for Brain tumor classification into four different types which is an important step in brain tumor diagnosis. Most of the recent research studies focus on binomial classification of brain MR image into tumorous and non-tumorous images that can be extracted using image segmentation. Further classification of the extracted tumor into various classes is an area that is yet to be explored. In our work, we propose an automated system to classify the segmented tumor into various classes. First, the wavelet features are extracted from all four MRI modalities (Flair, T1, T1c, T2) and an ensemble feature set is generated to perform the binomial classification using Random Forest trees. Next, tumor area is extracted from the classified tumorous images by using region growing image segmentation algorithm. In the final phase, wavelet features are extracted from the segmented parts and classification is performed for various tumor types (Necrosis, Edema, Enhancing and Non-Enhancing). The experiments are performed on 35 cases including 14 Low-Grade Glioma (LGG) and 21 High-Grade Glioma with total 21,700 MR images. An average accuracy of 94.33% for binomial MR image classification and 96.08% for multiclass tumor classification is achieved.

## Keywords

Brain MRI; Region Growing; Ensemble Wavelet Features; Tumor Segmentation; Multi-class Tumor Classification.

## 1. INTRODUCTION

In human brain, there are tissues known as “Glial” which are supportive tissues and keep the brain neurons in place and intact for functioning well. Any tumor which is caused by such tissues is termed as “Glioma”. This tumor mainly occurs in brain and spinal cord. The type of glioma tumor depends on the nature of glial cells involved. Gliomas has different types and each type have specific traits which could affect the brain function and could be life threatening [1]. Therefore it is necessary to classify the glioma type and location so that timely treatment and prognosis which may include chemotherapy, surgery or radiation therapy [2].

Although extensive research has been conducted in this field, still early diagnosis remained poor. The aggressive form of this disease termed as High Grade Gliomas (HGG) in which the survival rate is two or less number of years and immediate treatment is required [3]. There are Low Grade Gliomas (LGG), with slow growing rate and the life expectancy is several years. That's why the main focus is on these HGG which are heterogamous in nature with irregular shape and boundary but experiments are performed on both HGG and LGG. Furthermore the location and size vary considerably which makes the segmentation task more challenging [4]. This is a really crucial

task in order to follow up the treatment of HGG and LGG patient. The manual segmentation of such tumor through MR Imaging (MRI) is still a trusted process, performed by a neuro-radiologist. The MRI process is still preferred over other radiology methods as it is more accurate to locate the tumor cells [5]. But this manual process is very tedious and long, to alleviate such limitations, extensive research performed over automated brain tumor segmentation. Classification methods, which differentiate the tissues on intensity based, are discussed in [6]. Such methods are further categorized in to Supervised and Unsupervised classification methods. Supervised classifications methods need prior knowledge from training data sets and from this learning, algorithms take the decision. Still these training data sets are extensive and require time consuming pre-processing but produce better results. The working principle of such methods depends on imposing spatial coherence [7] or only knowledge regarding feature specification is required to perform the segmentation [8].

The tumor is classified in to different classes after segmentation. Different classification methods are discussed in [9], e.g. Multi-Layer Perceptron (MLP), Support Vector Machines (SVM), Radial Basis Function (RBF) and Random Forest (RF) Tree. These methods perform the classification by incorporating different tumor features. Most commonly used methods for feature extraction are Discrete Wavelet Transform (DWT), Discrete Fourier Transform (DFT) and Discrete Cosine Transform (DCT) [10]. The research article is structured as follows; in section 2, related work is discussed. In section 3, proposed system is described in details and section 4 discusses about experimental data, Section 5 confer the results and discussions and section 6 concludes the paper.

## 2. RELATED WORK

Because of the challenging nature of tumor segmentation problem, considerable research has been done for past 20 years which generated interactive, automatic and semi-automatic algorithms, presented in [11]. However, all these algorithms are tested over a relatively small database with different metrics of performance. Also the method validation was tested over varying combinations of imaging modalities. Therefore it remained difficult to judge the strategy and to pursue it further for clinical research. Most of the work has been done on the segmentation of the glioma tumor, e.g. presented in [12] and comparatively less research conducted on the multiclass tumor classification such as meningioma and other subtypes of glioma [13].

As stated earlier that methods can be divided in to supervised and unsupervised techniques. Supervised methods require prior knowledge of spatial distribution and appearance of tissues and exhibit better result at the cost of time consuming training on a data set. In training data set, the tumor can be modeled for

expected shape or the signal of image for a healthy tissue that is same as other techniques for brain lesions [14]. Sometimes a tumor specific ‘‘Bio Maker’’ is used to collect spatial prior for tumor [15] or from the images of patients estimate the localization of tumor structure [16]. The accuracy of all these models strictly rely on the alignment of images and spatial prior which of course is a critical task especially when large cavities and lesions are detected.

On other hand, unsupervised techniques learn directly the difference of characteristic between lesions and other tissues. At first, these techniques extract the vocal wise features from anatomical maps; this feature extraction can be done on basis of local intensity differences [17]. At next stage the classification algorithms will use these features to learn the class boundaries, using high dimensional feature space, and return the tumor classification map which can be used on new data set as well. These classification algorithms are based on support vector machines or decision trees [18].

Another type of unsupervised techniques is Fuzzy C-mean Clustering (FCM) for segmentation of brain tumor [19]. It assigns fuzzy membership to different tissue types by taking into account the overlapped classes of tissues. FCM was first used by Philips [20] in 1995 for brain tumor segmentation, later used with other techniques for better performance [21]. A supervised technique, Gaussian Mixture Model (GMM) has been presented in [6] by Menze, where the types of tissues are modeled by multi variant Gaussian distribution. The advanced MRI modalities can provide additional biological and structural information of tumors, which will make this segmentation task easier [22].

### 3. SYSTEM MODEL

The proposed method consists of multiple steps. In the initial phase, the input MR images having four different modalities, i.e. T1, T2, T1c and Flair, are processed using histogram matching and image normalization to enhance the image and remove noise. Next, DWT is applied on the preprocessed images to extract the textural features and form an ensemble feature set from all four modalities. Since tumor parts can have multiple classes, initially binomial classification using random forest classifier is performed to extract the tumorous and non-tumorous images. In the next step, region growing based image segmentation is applied to extract the tumor part from the tumorous images. For multiclass tumor classification, a three-level DWT is applied on the extracted tumor. The textural features of the tumor are used in the final step for tumor classification using RF. The RF classifier categorizes the tumor into four types, i.e. Necrosis, Edema, Enhancing and Non-Enhancing.

#### 3.1 Preprocessing

Brain MR images are captured in to commonly four modalities; T1, T2, T1c and FLAIR. Since the T1c has the highest spatial resolution, the remaining three modalities are co-registered with T1c to normalize the data. All the images are resampled to 1mm isotropic resolution by applying Linear interpolator [23]. The images are enhanced by applying the histogram matching using best contrast image in each modality as reference image [24].

#### 3.2 Feature Extraction (DWT)

Discrete Wavelet Transform (DWT) is a computationally inexpensive and effective method for decomposing an image into different sub-bands and extracting important textural features [25]. Single level DWT uses a low pass and a high pass filter to decompose the input data. In case of two-dimensional images, the

DWT is first applied to the rows of the input image and then to the columns. This results in the image decomposition into four sub-band coefficients that are called Low-Low (LL), Low-High (LH), High-Low (HL) and High-High (HH). From these sub-bands, the low-frequency coefficients LL are most valuable since they contain the smooth variations and approximations of the image. In this paper, for the features extraction, the image is decomposed into three levels by employing Daubechies wavelet filtering to extract the features [26]. In the first level, DWT is applied to get the four sub-bands. In the second level, DWT is applied further on the LL band of the first level to get further sub-bands of the image. Similarly, in the third level, the process is repeated and DWT is applied on the LL band from the second level to get more sub-band coefficients. The LL band coefficients at the third level contain the most important features.

A wavelet transform is the process of decomposition of input signal using wavelets. Continuous Wavelet Transform (CWT) and DWT use scaled and shifted versions of a finite length and fast decaying wavelet called the mother wavelet to extract the features of the input signal. The CWT of an input signal is its multiplication with the scaled and shifted wavelet function over time.

$$WT_x(a, \tau) = \frac{1}{\sqrt{a}} \int_{-\infty}^{+\infty} x(t) \Psi^*\left(\frac{t-\tau}{a}\right) dt \quad (1)$$

$$WT_x(a, \tau) = \langle x(t), \varphi_{a\tau}(t) \rangle \quad (2)$$

The function  $WT_x(a, \tau)$  contains different wavelet coefficients that represent the scaling and positioning information. In DWT, a discrete shifted version of the low pass scaling function  $\phi_{j,k}$  and a shifted version of bandpass wavelet function are used to calculate the decomposition of  $x(t)$  input signal.

$$x(t) = \sum_{k \in \mathbb{Z}} u_{j_0,k} \phi_{j_0,k}(t) + \sum_{j=-\infty}^{j_0} \sum_{k \in \mathbb{Z}} w_{j,k} \Psi_{j,k}(t) \quad (3)$$

In equation 3,  $w_{j,k}$  and  $u_{j,k}$  ( $j < j_0$ ) are the wavelet and scaling coefficients respectively.

$$u_{j,k} = \langle x, \phi_{j,k} \rangle, w_{j,k} = \langle x, \Psi_{j,k} \rangle \quad (4)$$

The scaling functions ( $\phi_{j,k}(t)$ ) and wavelet functions ( $\Psi_{j,k}(t)$ ) can be calculated from equations five and six respectively.

$$\phi_{j,k}(t) = 2^{-j/2} \phi\left(2^{-j/2}t - k\right) \quad (5)$$

$$\Psi_{j,k}(t) = 2^{-j/2} \Psi\left(2^{-j/2}t - k\right) \quad (6)$$

By using three-level DWT on the input MR images, the redundant feature set is reduced to a small set of discriminatory textural features. The output features vectors are of low dimension and are used to extract the characteristic features. The input MR image of is given as input. In the first level, LL sub-band produces image which is further reduced in the second level to . In the third level, sized approximation image is generated. In the next step, the approximation image is transformed into a singular matrix that contains the low-frequency coefficients that are sorted in the descending order. In the final step, top 36 values are selected as the feature set for each modality. The experiments are performed for each modality, and all four modalities features are ensemble into single feature set which increases the classifier accuracy significantly.

#### 3.3 Classification (Random Forest Trees)

In this work, several classifiers are tested for binomial MR image classification i.e. SVM, MLP, RBF, Naive Bayes, K-nearest

neighbors (KNN) and RF. From these classifiers, Naïve Bayes, KNN and RBF are discarded due to insufficient performance in the initial experiments. The results of the proposed work are compared with the RF, MLP and SVM classifiers. For binomial MR image classification, MLP produced highest accuracies for the ensemble based DWT features whereas, for Tumor classification, RF achieves the best accuracy.

Random forest classifier is used for the classification of tumorous and non-tumorous images [17]. In the initial phase of the algorithm, several decision trees are created randomly to form the forest. The decision trees are trained from randomly sampled data from the training dataset. The random forest classifier avoids overfitting the model by using a bootstrap aggregating (Bagging) technique [27]. The prediction with maximum votes is considered as the final outcome of the algorithm.

### 3.4 Brain Tumor Segmentation (Region Growing Based)

Segmentation in medical imaging is a challenging task. Region-based image segmentation produces better results compared to various measurement based methodologies [28]. Pixels in a specific region based on user criteria are used as seed points in region-based image segmentation. The region then grows to adjacent pixels iteratively based on different textural and intensity constraints. Selecting the accurate seed points that accurately describes the problem is an important factor in region-based image segmentation.

An automated procedure to generate edge-oriented seeds was introduced by Fan et al. in [29]. This method is applied to obtain a geometric structure of the input gray-scale image. From this geometric structure, the centroids of neighboring edges are used as input to the algorithm. K-means clustering algorithm is applied to generate a suitable number of clusters whose centers are used as seed pixels. K-means clustering technique partitions the input into K subgroups. In every iteration, the distance between the data points within a cluster is minimized and between data points of other clusters is maximized. The algorithm moves the centroid of each cluster to the average of the data points that fall in that set in the current iteration. The objective function in k-means is to minimize the sum of square error function defined in Eq. 7.

$$\text{Objective Function} = \sum_{j=1}^k \sum_{i=1}^n |x_i^j - \mu_j|^2 \quad (7)$$

$|x_i^j - \mu_j|^2$  is the distance between a data point  $x_i^j$ , and the cluster center  $\mu_j$  is an indicator of the distance of the  $n$  data points from their respective cluster centers. The roundness values of each extracted image are calculated to discard the out layer objects from the initial segmentation.

## 4. EXPERIMENTAL DATASET

The proposed system is tested on BraTS benchmarked dataset [6]. The dataset provide by MICCAI is online available for research purpose. It consists on LGG and HGG cases of four MRI sequence types including T1, T2, T1c and Flair. The training datasets also contains the ground truth annotated images for each case. Due to high processing power required, we performed testing on 14 LGG cases and 21 HGG cases totaling 21,700 MR images. From the BraTS dataset 2015 a total of 35 cases were chosen consisting of 21 High Grade Glioma (HGG) and 14 cases of Low Grade Glioma (LGG). Each case consisted of 4 types of modalities namely; T1, T2, T1c and Flair. Additionally, cases with Glioma tumor have been classified into 4 classes; Necrosis, Edema, Enhancing and Non Enhancing. The fifth class is that of

No Glioma tumor. The total number of MR images were 21,700 divided into 13,020 HGG cases and 8,680 LGG cases. 36 wavelet features were used for identification of tumor and again 36 features were extracted from the segmented tumor to identify the class of the tumor. Experiments are performed by randomly splitting the datasets into 80% for training and using 20% for testing.

## 5. RESULTS AND EVALUATION

The proposed method was tested on the dataset listed above in order to validate the method. As previously mentioned, the set consists of 21,700 MR images divided into 13,020 MR images for LGG cases and 8,680 MR images for LGG cases. After the preprocessing phase, the images classified into tumorous and non-tumorous based on the extracted wavelet features. To classify the images, three classifiers were used namely; Support Vector Machines (SVM), Random Forest (RF) and Multi-Layer Perceptron (MLP). Table 2 describes the classification results for all four modality types individually and ensemble all modality types features for both LGG and HGG. In both cases of LGG and HGG, the MLP achieved the highest accuracy in classification with an overall accuracy of 92.92% for LGG and 94.33% for HGG. The RF classifier achieved a high average accuracy but did not perform as well as the MLP. The lower accuracy for LGG is expected since the shape and size of tumor features which makes the process more difficult as compared to HGG.

After classification, the tumorous portion of the MR images need to be segmented. In this regard, a novel segmentation method is proposed to isolate the tumorous portion of the brain by discarding non-tumorous images. Table 3 below shows the results of segmentation for the tumorous images. As shown, the proposed method achieved an average accuracy of 93.22% as compared to the normal full MR image input based segmentation method which achieves only 78.9% accuracy. Average specificity of the proposed segmentation technique was 99.86% as compared to the full MR image based that only achieved 87.22% specificity. Other variables such as sensitivity, DSC, and MI were all significantly higher in the proposed segmentation technique achieving an average of 95.52%, 90.87%, and 86.49% respectively.

Figure 1 shows the image segmentation results for some samples. As can be seen, the images are first manipulated by changing the intensity values (column A) to enhance the tumorous portions of the image. The image is then put through the proposed initial segmentation method and the extracted cluster's shape roundness values are calculated (column B). The proposed segmentation method utilizing the region growing method is then applied to enhance the tumor segment. The boundaries of the tumorous portion of the image are then highlighted as shown in (column C). To validate our results for the segmentation portion, we included the actual tumor segment as part of the BRaTS annotated dataset Column D). It can be observed that the proposed segmentation technique was highly efficient and achieved a high accuracy of 93.22%.

**Table 1. Binomial Classification Accuracies Comparison**

Modality	LGG			HGG		
	SVM	RF	MLP	SVM	RF	MLP
Flair	82.15	80.74	83.57	89.79	89.41	91.49
T1	68.27	75.64	76.20	74.67	75.61	76.37
T1c	67.14	75.35	76.20	73.54	75.24	79.58
T2	75.07	79.60	80.45	82.42	85.82	86.58
Combined	87.82	92.64	92.92	91.49	92.63	94.33

**Table 2. Comparison of Tumor Segmentation Results**

Data Source	MICCAI BraTS 2015	
	Proposed Tumor Extracted	Full Image Based
Accuracy	93.22 %	78.92%
Specificity	99.86%	87.22%
Sensitivity	95.52%	81.29%
DSC	90.87%	74.50%
MI	86.49%	66.86 %

There are different classes of Glioma and the complete system proposed in this paper is not only able to classify tumorous and non-tumorous image and segment them, but it is able to classify tumorous images into the different types (classes) of Glioma cancer based on the proposed extracted features (36 wavelet features) of the segmented image. The four classes of Glioma cancer are Necrosis, Edema, enhancing and non-enhancing. As shown in Table 4, the three classifiers SVM, MLP and RF were used for classification of the tumorous images into the four classes for both LGG and HGG. The proposed method was applied on both Full Images and Extracted (Segmented) Images. In all four classes, it can be seen that the Random Forest (RF) achieved the greatest accuracy. RF achieved an average accuracy of 96.66% to identify the tumor as Necrosis, 100% in identifying the tumor as Edema, 93.38% as enhancing, and 97.24% as non-enhancing. It can be observed that these high classification accuracies are achieved on the images where the tumor has been extracted by the proposed method in this paper. The average accuracy for achieved on the extracted tumor images are higher than of those achieved in previous literature. The average accuracy in classifying the extracted tumor to the Necrosis class is 94.28%, 99.81% to Edema Class, 93.95% to the enhancing class, and finally 92.06% to the non-enhancing class. The automatic recognition and subsequent classification of the Glioma tumor in MR images is thus achieved through the novel methods proposed in this paper.

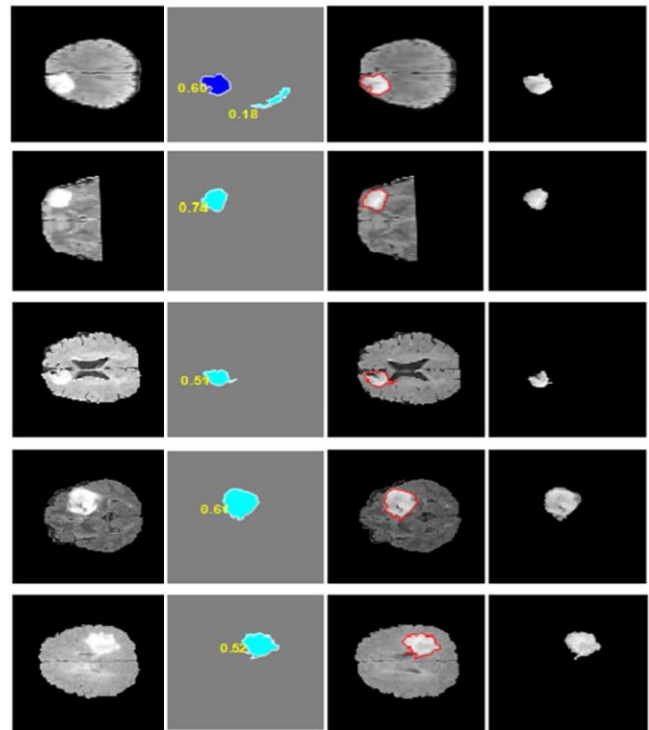


**Figure 1. Experiment results of tumor segmentation samples of BraTS Datasets. Each row representing different patient MR Images. (Col. A). Preprocessed enhanced MR Images, (Col. B). Applied proposed initial segmentation method and extracted clusters shape roundness values, (Col. C). Highlighted boundary of the enhanced tumor segments, (Col. D). Annotated tumor segment for the corresponding image.**

**Table 3. Tumor Class based Classification Results**

		SVM ( $\pm 0.30$ %)				MLP ( $\pm 0.25$ %)				RF ( $\pm 0.20$ %)			
		Full Image		Tumor Extracted		Full Image		Tumor Extracted		Full Image		Tumor Extracted	
	Modality	HGG	LGG	HGG	LGG	HGG	LGG	HGG	LGG	HGG	LGG	HGG	LGG
<b>Necrosis</b>	Flair	81.29	78.47	91.49	94.47	90.74	84.70	94.14	93.32	92.25	86.97	95.09	96.08
	T1	72.97	78.47	92.25	94.47	74.86	77.90	92.63	93.55	74.48	75.35	93.76	97.24
	T1c	84.31	78.47	91.30	94.47	89.41	69.41	94.71	96.08	88.66	76.77	93.76	97.01
	T2	81.10	85.84	91.87	94.70	83.18	87.25	93.01	96.08	86.20	87.82	94.52	96.31
	<b>Average</b>	<b>79.92</b>	<b>80.31</b>	<b>91.72</b>	<b>94.53</b>	<b>84.55</b>	<b>79.82</b>	<b>93.62</b>	<b>94.76</b>	<b>85.40</b>	<b>81.73</b>	<b>94.28</b>	<b>96.66</b>
<b>Edema</b>	Flair	89.98	82.15	97.54	97.01	91.30	83.57	99.43	99.31	90.17	81.30	99.81	100.00
	T1	74.48	68.27	97.54	97.01	76.56	76.20	99.43	99.31	76.56	74.22	99.81	100.00
	T1c	73.54	67.14	97.54	97.01	79.21	76.20	99.43	99.31	77.13	75.64	99.81	100.00
	T2	82.61	75.07	97.54	97.01	86.01	80.45	99.43	99.31	85.26	80.17	99.81	100.00
	<b>Average</b>	<b>80.15</b>	<b>73.16</b>	<b>97.54</b>	<b>97.01</b>	<b>83.27</b>	<b>79.11</b>	<b>99.43</b>	<b>99.31</b>	<b>82.28</b>	<b>77.83</b>	<b>99.81</b>	<b>100.00</b>
<b>Non Enhancing</b>	Flair	85.26	82.44	92.82	89.86	90.36	84.42	93.76	89.40	89.79	87.54	93.01	93.09
	T1	68.24	82.44	92.63	91.01	71.46	81.02	93.76	90.78	73.91	78.19	93.95	93.32
	T1c	76.94	82.44	92.63	91.24	84.69	76.77	93.38	92.86	79.96	79.04	94.71	94.01
	T2	82.99	88.10	92.82	88.94	85.44	92.07	93.76	91.71	86.20	91.79	94.14	93.09
	<b>Average</b>	<b>78.36</b>	<b>83.85</b>	<b>92.72</b>	<b>90.27</b>	<b>82.99</b>	<b>83.57</b>	<b>93.67</b>	<b>91.19</b>	<b>82.47</b>	<b>84.14</b>	<b>93.95</b>	<b>93.38</b>
<b>Enhancing</b>	Flair	85.07	85.55	91.68	96.77	88.28	86.40	91.87	96.08	89.60	86.12	90.93	97.00
	T1	63.52	66.29	91.87	96.54	67.86	70.26	92.82	96.54	72.78	69.69	92.44	98.16
	T1c	80.15	62.89	92.63	96.77	86.58	70.54	91.12	95.62	82.99	71.96	92.44	97.24
	T2	82.80	75.07	91.68	96.54	84.12	78.75	92.06	96.31	83.93	78.19	92.44	96.54
	<b>Average</b>	<b>77.88</b>	<b>72.45</b>	<b>91.97</b>	<b>96.66</b>	<b>81.71</b>	<b>76.49</b>	<b>91.97</b>	<b>96.14</b>	<b>82.32</b>	<b>76.49</b>	<b>92.06</b>	<b>97.24</b>

## 6. CONCLUSION

This research work focuses an automated system to segment and classify the tumor into multiple classes that can help the radiologists for accurate and early diagnosis of the brain tumor. The process classifies and extracts the tumor part of the image using binomial classification and image segmentation respectively. The tumor area is further categorized into four different tumor classes. For experiments, BRATS brain MRI dataset is used, and results are produced based on the various classifiers. The experimental results show that for multiclass tumor classification, an accuracy of 96.82% and 95.03% is achieved for LGG and HGG respectively. For the binomial brain MR image classification an accuracy of 94.33% is attained while for the segmentation of tumorous part from the image, 93.22% accuracy is acquired having specificity and sensitivity of 99.86% and 95.52% respectively.

## 7. REFERENCES

- [1] Hsieh, Kevin Li-Chun, Chung-Ming Lo, and Chih-Jou Hsiao. "Computer-aided grading of gliomas based on local and global MRI features." *Computer Methods and Programs in Biomedicine* 139 (2017): 31-38.
- [2] Wen, Patrick Y., David R. Macdonald, David A. Reardon, Timothy F. Cloughesy, A. Gregory Sorensen, Evanthia Galanis, John DeGroot et al. "Updated response assessment criteria for high-grade gliomas: response assessment in neuro-oncology working group." *Journal of Clinical Oncology* 28, no. 11 (2010): 1963-1972.
- [3] Louis, David N., Hiroko Ohgaki, Otmar D. Wiestler, Webster K. Cavenee, Peter C. Burger, Anne Jouvett, Bernd W. Scheithauer, and Paul Kleihues. "The 2007 WHO classification of tumours of the central nervous system." *Acta neuropathologica* 114, no. 2 (2007): 97-109.
- [4] Sauwen, Nicolas, M. Acou, S. Van Cauter, D. M. Sima, J. Veraart, F. Maes, Uwe Himmelreich, E. Achten, and Sabine Van Huffel. "Comparison of unsupervised classification methods for brain tumor segmentation using multi-parametric MRI." *NeuroImage: Clinical* 12 (2016): 753-764.
- [5] Giedd, Jay N. "Structural magnetic resonance imaging of the adolescent brain." *Annals of the New York Academy of Sciences* 1021 no. 1 (2004): 77-85.
- [6] Menze, Bjoern H., Andras Jakab, Stefan Bauer, Jayashree Kalpathy-Cramer, Keyvan Farahani, Justin Kirby, Yuliya Burren et al. "The multimodal brain tumor image segmentation benchmark (BRATS)." *IEEE transactions on medical imaging* 34, no. 10 (2015): 1993-2024.
- [7] Nie, Jingxin, Zhong Xue, Tianming Liu, Geoffrey S. Young, Kian Setayesh, Lei Guo, and Stephen TC Wong. "Automated brain tumor segmentation using spatial accuracy-weighted hidden Markov Random Field." *Computerized Medical Imaging and Graphics* 33, no. 6 (2009): 431-441.
- [8] Kazerooni, Anahita Fathi, Meysam Mohseni, Sahar Rezaei, Gholamreza Bakhshandehpour, and Hamidreza Saligheh Rad. "Multi-parametric (ADC/PWI/T2-w) image fusion approach for accurate semi-automatic segmentation of tumorous regions in glioblastoma multiforme." *Magnetic Resonance Materials in Physics, Biology and Medicine* 28, no. 1 (2015): 13-22.
- [9] [10]. Bauer, Stefan, Roland Wiest, Lutz-P. Nolte, and Mauricio Reyes. "A survey of MRI-based medical image analysis for brain tumor studies." *Physics in medicine and biology* 58, no. 13 (2013): R97.
- [10] Latif, G., Butt, M. M., Khan, A. H., Butt, O., & Iskandar, D. A. (2017, April). Multiclass brain Glioma tumor classification using block-based 3D Wavelet features of MR images. In *Electrical and Electronic Engineering (ICEEE), 2017 4th International Conference on* (pp. 333-337). IEEE.
- [11] Angelini, Elsa D., Olivier Clatz, Emmanuel Mandonnet, Ender Konukoglu, Laurent Capelle, and Hugues Duffau. "Glioma dynamics and computational models: a review of segmentation, registration, and in silico growth algorithms and their clinical applications." *Current Medical Imaging Reviews* 3, no. 4 (2007): 262-276.
- [12] Latif, G., Iskandar, D. A., Jaffar, A., & Butt, M. M. (2017). Multimodal Brain Tumor Segmentation using Neighboring Image Features. *Journal of Telecommunication, Electronic and Computer Engineering (JTEC)*, 9(2-9), 37-42
- [13] Weizman, Lior, L. Ben Sira, Leo Joskowicz, Shlomi Constantini, Ronit Precel, Ben Shofty, and D. Ben Bashat. "Automatic segmentation, internal classification, and follow-up of optic pathway gliomas in MRI." *Medical image analysis* 16, no. 1 (2012): 177-188.
- [14] Seghier, Mohamed L., Anil Ramlackhansingh, Jenny Crinion, Alexander P. Leff, and Cathy J. Price. "Lesion identification using unified segmentation-normalisation models and fuzzy clustering." *Neuroimage* 41, no. 4 (2008): 1253-1266.
- [15] Moon, Nathan, Elizabeth Bullitt, Koen Van Leemput, and Guido Gerig. "Model-based brain and tumor segmentation." In *Pattern Recognition, 2002. Proceedings. 16th International Conference on*, vol. 1, pp. 528-531. IEEE, 2002.
- [16] Gooya, Ali, Kilian M. Pohl, Michel Bilello, Luigi Cirillo, George Biros, Elias R. Melhem, and Christos Davatzikos. "GLISTR: glioma image segmentation and registration." *IEEE transactions on medical imaging* 31, no. 10 (2012): 1941-1954.
- [17] Geremia, Ezequiel, Bjoern H. Menze, and Nicholas Ayache. "Spatially adaptive random forests." In *Biomedical Imaging (ISBI), 2013 IEEE 10th International Symposium on*, pp. 1344-1347. IEEE, 2013.
- [18] A. Criminisi and J. Shotton, "Decision Forests for Computer Vision and Medical Image Analysis". Heidelberg, Germany: Springer, 2013.
- [19] Gordillo, Nelly, Eduard Montseny, and Pilar Sobrevilla. "State of the art survey on MRI brain tumor segmentation." *Magnetic resonance imaging* 31, no. 8 (2013): 1426-1438.
- [20] Phillips, W. E., R. P. Velthuizen, S. Phuphanich, L. O. Hall, L. P. Clarke, and M. L. ilbiger. "Application of fuzzy c-means segmentation technique for tissue differentiation in MR images of a hemorrhagic glioblastoma multiforme." *Magnetic resonance imaging* 13, no. 2 (1995): 277-290.
- [21] Fletcher-Heath, Lynn M., Lawrence O. Hall, Dmitry B. Goldgof, and F. Reed Murtagh. "Automatic segmentation of non-enhancing brain tumors in magnetic resonance images." *Artificial intelligence in medicine* 21, no. 1 (2001): 43-63.
- [22] Cha, S. "Update on brain tumor imaging: from anatomy to physiology." *American Journal of Neuroradiology* 27, no. 3 (2006): 475-487.
- [23] Padhani, Anwar R., and Kenneth A. Miles. "Multiparametric imaging of tumor response to therapy 1." *Radiology* 256, no. 2 (2010): 348-364.
- [24] Wang, H., & Zhang, P. (2015). The Research Of Mapping Laws For Image Histogram Matching.
- [25] Babu, G., & Sivakumar, R. (2017, June). Comparative Analysis of MRI-PET Brain Image Fusion Using Discrete Wavelet Transform. In *Proceedings of the International Conference on Graphics and Signal Processing* (pp. 48-54). ACM.
- [26] Singh, R., & Khare, A. (2014). Fusion of multimodal medical images using Daubechies complex wavelet transform—A multiresolution approach. *Information Fusion*, 19, 49-60.
- [27] Hegde, C., Wallace, S., & Gray, K. (2015, September). Using trees, bagging, and random forests to predict rate of penetration during drilling. In *SPE Middle East Intelligent Oil and Gas Conference and Exhibition*. Society of Petroleum Engineers
- [28] Wang, L., Wu, H., & Pan, C. (2013). Region-based image segmentation with local signed difference energy. *Pattern Recognition Letters*, 34(6), 637-645.
- [29] Fan, J., Zeng, G., Body, M., & Hacid, M. S. (2005). Seeded region growing: an extensive and comparative study. *Pattern recognition letters*, 26(8), 1139-1156.

## Authors' background

Your Name	Title*	Research Field	Personal website
Ghazanfar Latif	Instructor, Senior PhD candidate	Medical Image Processing, Machine Learning, Decision Systems, Big Data	
D.N.F. Awang Iskandar	Associate Research Dean, Faculty of Computer Science and Information Technology, PhD	Machine Learning, Image Processing, Semantic Technologies	
Jaafar Alghazo	Dean, College of Computer Engineering and Sciences, PhD	Machine Learning, Artificial Intelligence, Embedded Systems, Image Processing	

\*This form helps us to understand your paper better, **the form itself will not be published.**

\*Title can be chosen from: master student, Phd candidate, assistant professor, lecture, senior lecture, associate professor, full professor